Universiteit Leiden
The Netherlands

Simulation of 1/f charge noise affecting a quantum dot in a Si/SiGe structure

Kępa, M.; Focke, N.; Cywiński, Ł.,; Krzywda, J. A.

Citation
Kępa, M., Focke, N., Cywiński, Ł. ,, & Krzywda, J. A. (2023). Simulation of 1/f charge noise affecting a quantum dot in a Si/SiGe structure. *Applied Physics Letters*, *123*(3). doi:10.1063/5.0151029

Version: Publisher's Version
License: Licensed under Article 25fa Copyright Act/Law (Amendment Taverne)
Downloaded from: https://hdl.handle.net/1887/3718715

Note: To cite this publication please use the final published version (if applicable).

Applied Physics Letters

RESEARCH ARTICLE | JULY 19 2023

Simulation of $1/f$ charge noise affecting a quantum dot in a Si/SiGe structure

Special Collection: Electronic Noise: From Advanced Materials to Quantum Technologies

M. Kępa ; N. Focke ; Ł. Cywiński ; J. A. Krzywda

Check for updates

Appl. Phys. Lett. 123, 034005 (2023)
https://doi.org/10.1063/5.0151029

View Online
Export Citation
CrossMark

06 March 2024 09:20:08

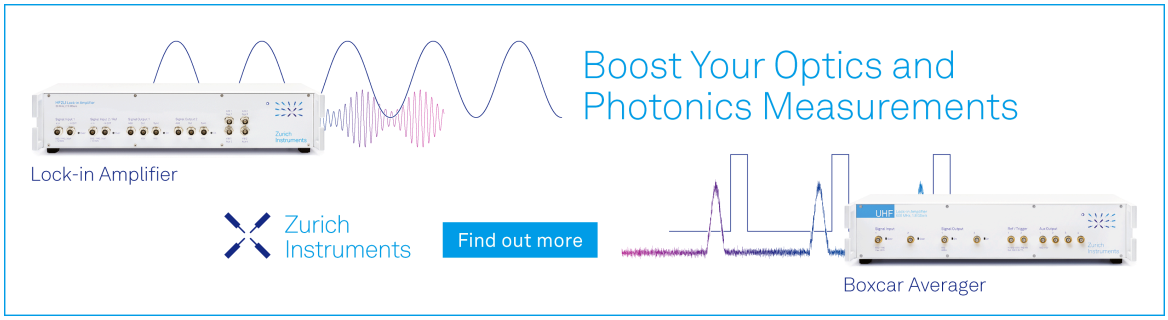

AIP Publishing

Applied Physics Letters ARTICLE pubs.aip.org/aip/apl

Simulation of $1/f$ charge noise affecting a quantum dot in a Si/SiGe structure

Cite as: Appl. Phys. Lett. **123**, 034005 (2023); doi: 10.1063/5.0151029
Submitted: 17 March 2023 · Accepted: 27 June 2023 ·
Published Online: 19 July 2023

View Online Export Citation CrossMark

M. Kępa,[1] N. Focke,[2] Ł. Cywiński,[1] and J. A. Krzywda[1,3,a)]

AFFILIATIONS

[1]Institute of Physics, Polish Academy of Sciences, al. Lotników 32/46, PL 02-668 Warsaw, Poland
[2]JARA-FIT Institute for Quantum Information, Forschungszentrum Jülich GmbH and RWTH Aachen University, Aachen, Germany
[3]Lorentz Institute and Leiden Institute of Advanced Computer Science, Leiden University, P.O. Box 9506, 2300 RA Leiden, The Netherlands

Note: This paper is part of the APL Special Collection on Electronic Noise: From Advanced Materials to Quantum Technologies.
[a)]**Author to whom correspondence should be addressed:** krzywda@ifpan.edu.pl

ABSTRACT

Due to presence of magnetic field gradient needed for coherent spin control, dephasing of single-electron spin qubits in silicon quantum dots is often dominated by $1/f$ charge noise. We investigate theoretically fluctuations of ground state energy of an electron in gated quantum dot in a realistic Si/SiGe structure. We assume that the charge noise is caused by motion of charges trapped at the semiconductor–oxide interface. We consider a realistic range of trapped charge densities, $\rho \sim 10^{10}$ cm^{-2}, and typical lenghtscales of isotropically distributed displacements of these charges, $\delta r \leq 1$ nm, and identify pairs $(\rho, \delta r)$ for which the amplitude and shape of the noise spectrum are in good agreement with spectra reconstructed in recent experiments on similar structures.

Published under an exclusive license by AIP Publishing. https://doi.org/10.1063/5.0151029

06 March 2024 09:20:08

Charge noise with $1/f$ spectrum is ubiquitous in semiconductor nanostructures.[1–4] In gate-defined quantum dots (QDs),[5] this noise is probably caused by bistable sources of electric fields localized at the semiconductor/insulator interface, or within the insulator separating semiconducting material from the gate.[6–9] Spins of electrons or holes confined in QDs have been demonstrated to be viable qubits,[10,11] with the gated QD architectures showing constant progress toward scalable multi-qubit devices.[12,13] While using the spin of a single electron as the qubit makes its quantum state insensitive, to the first order, to charge noise, decoherence caused by that noise is relevant for operation of two-qubit gates[14–17] and evolution of singlet–triplet qubits based on two electrons in two QDs.[18–25] Moreover, charge noise has been recently recognized as the factor limiting the quality of single-spin qubits in silicon-based QDs.[26–28] This is due to presence of either real[29–31] or artificial spin–orbit couplings caused by presence of magnetic field gradients, which are necessary for single-qubit operations.[16,26,32–34]

The microscopic sources of charge noise in gated QD architectures have not been fully characterized yet. However, recent progress in reconstruction of spectra of $1/f$ charge noise affecting the QDs[22,27,35,36] has provided many experimental data against which one could test various models of these sources. It is now known that the power spectral density (PSD) of noise of electronic energy levels in a typical QD has $1/f$ form for $f \in [10^{-3}, 10^{6}]$ Hz (and possibly in an even broader range), albeit with visible deviations from ideal $1/f$ scaling, and the typical amplitude of noise at 1 Hz is of the order of 1 μeV/$\sqrt{\text{Hz}}$ for electrons in Si/SiGe,[5,22,27,37,38] while being within one order of magnitude from this value for any other characterized spin qubit, see Ref. 5 and references therein.

In recent papers, modeling of charge noise was performed for electron[39] and hole[40] spin qubits in SiMOS devices. Here, we focus on electron spin qubits in Si/SiGe devices of the type used in recent experiments on electron spin qubit shuttling.[41,42] We assume that the noise is caused by sub-nm motion of charges trapped at the Si/SiO_2 interface[42–47] that have density $\rho_{\text{ic}} \sim 10^{10}$ cm^{-2}. Simulations in Ref. 42 showed that using $\rho_{\text{ic}} = 5 \times 10^{10}$ cm^{-2} reproduces typically observed electrostatic-disorder-induced energy detunings between neighboring QDs. Focusing on ρ_{ic} in the range from 5×10^{9} cm^{-2} to 10^{11} cm^{-2}, we calculate the influence of these charges on the ground-state (GS) orbital energy of an electron in a QD in the considered nanostructure. We then investigate what typical length scale of isotropic charge motion and charge densities lead to reproduction of measured shape and amplitude of $1/f$-like noise spectra.

We employ the simplest model leading to $1/f$ noise spectrum: that of many *independent* sources of random telegraph noise

Published under an exclusive license by AIP Publishing

(RTN)[8,48,49]—the so-called two-level fluctuators (TLFs)—having switching rates γ drawn from a lognormal distribution spanning over many orders of magnitude of γ.[50–53] We consider here noise at fixed temperature, i.e., $T \approx 100$ mK at which spin qubits are typically operated and assume equal average occupations of each state of a TLF. This means without considering the origin of TLFs dynamics (see, e.g., Refs. 54 and 55 for discussion of some of the models). Distinct electric fields generated by the TLF in each of its states cause state-dependent shifts of ground state energy of the nearby QD. We define the coupling of the QD to the nth TLF, η_n, as the shift of the energy of the GS orbital of an electron in the QD caused by a switching of the TLF. We focus on switching events that correspond to a sub-nm motion of a defect charge in the insulating layer between the semiconductor and the metallic gate (the blue region in Fig. 1). The two locations of the charge corresponding to the two states of the nth TLF are $\mathbf{r}_n$ and $\mathbf{r}_n + \delta\mathbf{r}_n$. We have checked that charge tunneling between the insulator and the metal leads to shifts of energy levels of the QD that are too large to be reconciled with the experimentally observed noise levels, unless defect is less than 0.2 nm away from the metal. As the tunneling events were also excluded as a source of charge noise in similar analysis performed for SiMOS devices,[39] here we only take into account the motion of defect localized at the semiconductor–oxide interface.

The PSD of the noise in GS energy of the electron in the QD is given by a sum of Lorentzian PSDs of the RTNs,

$$S(f) = \sum_{n=1}^{N} \frac{2\eta_n^2}{\gamma_n + (2\pi f)^2/\gamma_n}. \quad (1)$$

For a large number of TLFs, a flat distribution of η_n and a lognormal distribution of γ_n, i.e., $p(\gamma_n) \propto 1/\gamma_n$, result in the PSD that is well approximated by the 1/f noise spectrum, i.e., $S(f) \approx S_1 f_1/f$, where S_1 is the power of the noise at $f_1 = 1$ Hz, which is of the order of 1 μeV^2/Hz in state-of-the-art Si/SiGe QDs.[56]

We consider a realistic Si/SiGe device based on Refs. 41 and 42. We show its Computer Aided Design (CAD) model in Fig. 1(a). The structure consists of a quantum well (pink) that has two $Si_{0.7}Ge_{0.3}$ layers with a 10 nm thick Si layer in between. On top, there are 13 electrodes (yellow, red), to which voltages are applied. We use a gate pitch of 60 nm, and the width of each gate is set to 50 nm, which are within the range considered in Ref. 42. In this design, we have a 10 nm screening layer (green) that is insulated from the quantum well and the electrodes by another 10 nm of the oxide layer (blue), followed by a 1.5 nm Si Cap layer. We use $\epsilon_r = 3.9$ for the relative permittivity of the SiO_2 oxide. We define a channel as a gap in the screening layer, which allows the electric field to penetrate the structure and define the QDs about 80 nm below the terminal. We set $d_{\text{Channel}} = 200$ nm as in Refs. 42 and 57. The remaining dimensions are given in the caption of Fig. 1(a). The device structure and dimensions are similar to those of experimentally studied QDs,[22,58–61] although except for Ref. 61 plunger and barrier gates tend to be located on separate layers. We neglect any influence of electron reservoirs, as due to possibility of charge shuttling,[41,42] they can be located sufficiently far from the QDs used to host the qubits.

We consider a single QD defined under the central gate (red). We solve for electrostatic potential with voltages set on the electrodes, and we then find the electron GS energy, E_0, by solving the three-dimensional Schroedinger equation for the envelope function in the 10 nm Si layer. We have used single-band effective mass approximation

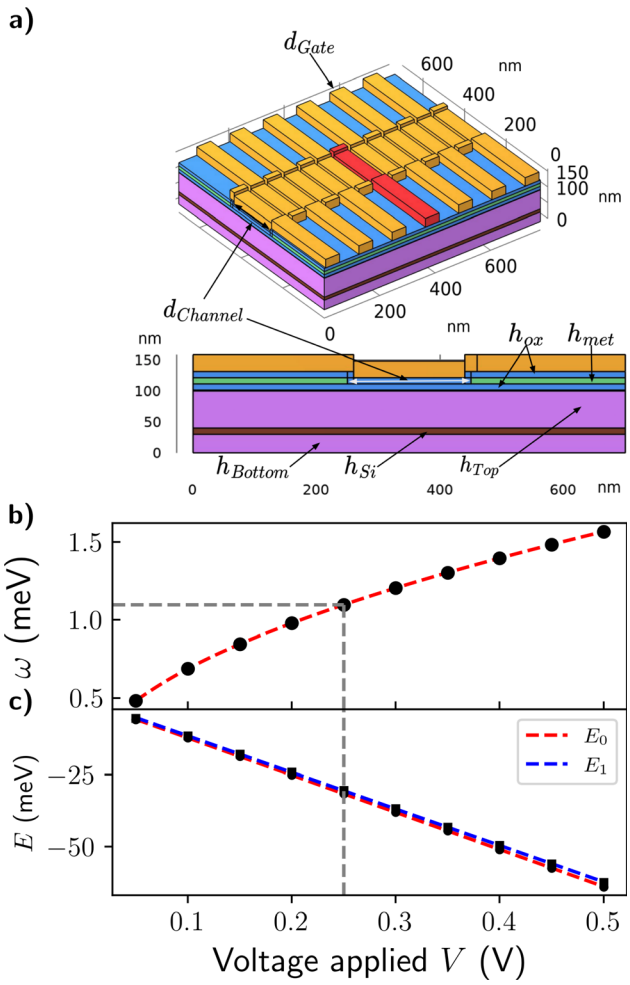

FIG. 1. (a) CAD model of the device. Electrodes that define the potential located on top of the device are separated from the bulk structure with conductive and insulating oxide layers. $d_{Gate} = 50$ nm, $d_{Channel} = 60$ nm, $h_{Top} = 60$ nm, $h_{Si} = 10$ nm, $h_{Bottom} = 30$ nm. (b) Orbital gap $\omega = E_1 - E_2$ as a function of applied voltage with interpolated trend line. Gray dashed line marks $V = 0.25$ V that corresponds to $\omega \approx 1.1$ meV, which is used in all further simulations. (c) The dependence of individual energy levels along with lever arm fits with $\alpha_0 = -128.86$ meV/V and $\alpha_1 = -126.54$ meV/V.

and omitted spin and valley degrees of freedom. We characterize the QD in Figs. 1(b) and 1(c), where the orbital gap and energies of the two lowest orbitals are shown as a function of the voltage applied to central gate, V, while keeping the other gates grounded. We choose $V = 0.25$ V giving a realistic orbital gap $\omega = E_1 - E_0 \approx 1.1$ meV.

We assume that the charge noise is generated by the motion of negative charges close to the semiconductor/oxide interface about 60 nm above the Si quantum well, i.e., on the upper surface of pink block at $z_0 \approx 100$ nm in Fig. 1(a). A charge at $\mathbf{r}_n = (x_n, y_n, z_0)$ shifts the GS of the electron by $\delta E(\mathbf{r}_n) = E_0' - E_0$, where E_0', E_0 are the GS energies with and without the charge present, respectively. To compute this shift, we insert a point charge $(-|e|)$ at $\mathbf{r}_n = (x_n, y_n, z_0)$ and repeat the procedure described above: compute the electrostatic

06 March 2024 09:20:08

Published under an exclusive license by AIP Publishing

potential and find the new GS energy $E_0' = E_0 + \delta E(\mathbf{r}_n)$. In Fig. 2(a), we plot $\delta E(\mathbf{r}_n)$ for the device shown in Fig. 1. We assume that the charges are located near the $z_0 = 102$ nm plane, i.e., 0.5 nm above the interface between the oxide and the Si cap layer. The results for $A = 600 \times 600\,\mathrm{nm}^2$ region are obtained using COMSOL software, with a regular grid of 31×31 charge positions in the plane. We have checked that shifts from two charges localized at $\mathbf{r}_n$ and $\mathbf{r}_m$ are approximately additive, i.e., $\delta E(\mathbf{r}_n, \mathbf{r}_m) \approx \delta E(\mathbf{r}_n) + \delta E(\mathbf{r}_m)$ within a 2% relative error.

To model a single TLF, we add a random displacement of the charge position, $\delta\mathbf{r}_n$, that causes an additional shift in the GS energy (see Fig. 2), given by

$$\eta_n = \delta E(\mathbf{r}_n + \delta\mathbf{r}_n) - \delta E(\mathbf{r}_n), \tag{2}$$

defining the coupling between the TLF and the QD. As the relative energy shifts due to $|\delta\mathbf{r}_n| < 1$ nm are small, we approximate the coupling by

$$\eta_n \approx \nabla\delta E(\mathbf{r}_n) \cdot \delta\mathbf{r}_n, \tag{3}$$

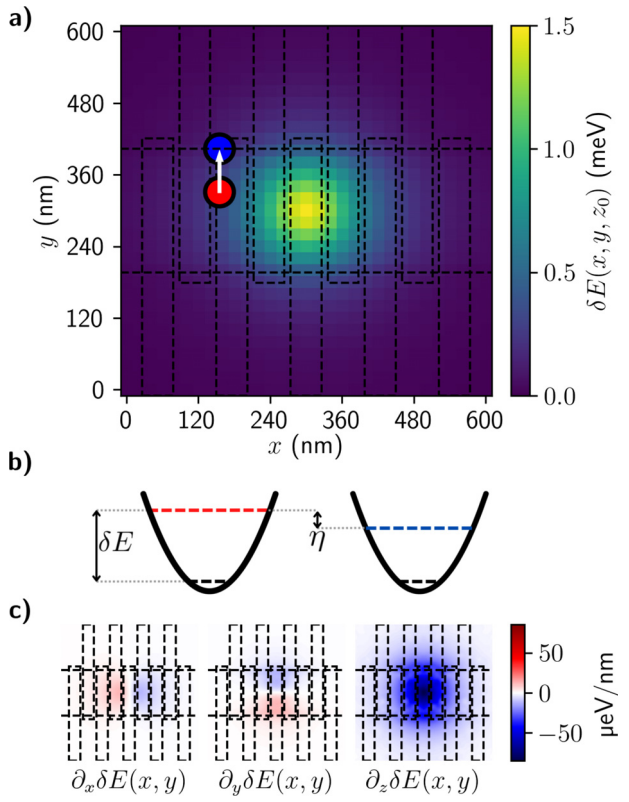

FIG. 2. Results of the finite-element method implemented in COMSOL. (a) Shift of ground state energy $\delta E(\mathrm{r})$ due to charge defect located at $\mathrm{r} = (x, y, z_0)$, where $z_0 = 102$ nm [see Fig. 1(a)]. (b) Illustration of the energy shift δE (left) caused by the presence of a point charge, and additional shift η (right) caused by a displacement of this charge from red to blue point in panel (a). We exaggerate the displacement size for illustration purposes. (c) Interpolated spatial derivatives of $\delta E(\mathbf{r})$ along all three dimensions.

where $\nabla = (\partial_x, \partial_y, \partial_z)$. In Fig. 2(c), we show the components of $\nabla\delta E(\mathbf{r})$, generated from interpolated $\delta E(\mathbf{r})$. For slowly varying x and y derivatives, we interpolate results from Fig. 2(a). For z derivative, we interpolate results obtained at $z_0 = 101.75, 102.0, 102.25, 102.5$ nm planes.

The motion of the charge away from the dot leads to a decrease in $\delta E(\mathbf{r})$, i.e., $\eta < 0$. In the xy plane, this is due to change in a distance between the defect and a QD, which leads to $|\partial_{x,y}\delta E(\mathbf{r})| \approx 10\ \mu$eV/nm in the central region of <100 nm from the dot. The motion toward and away from the dot results in the opposite sign of x and y derivatives on the two sides of the QD center. On the other hand, the derivative in z direction is always negative and about an order of magnitude larger, as it is related to a decrease in the distance between the defect and metallic layer, i.e., a decrease in a dipole moment of the electron and its mirror charge in the metallic gate. As a result, $\partial_z\delta E(\mathbf{r}) \approx 50\ \mu$eV/nm in the central region of ≈ 100 nm radius, in which $\delta E(\mathbf{r})$ is significant. Outside of this region $\partial_z\delta E(\mathbf{r})$ decays toward $\approx 0.5\ \mu$eV/nm at the edge of the considered region A. This shows that the TLFs outside of A do not contribute significantly to the energy shift.

We compute the PSD of total noise by adding contributions of all the TLFs, each given by Eq. (1). This approach is consistent with $\eta_n \ll \delta E(\mathbf{r}_n)$ and additivity of $\delta E(\{\mathbf{r}\})$, which has been tested for two charges. We define N as the number of TLFs that are active, i.e., having their γ_n in the range of frequencies $[f_{\min}, f_{\max}]$. We choose this range as 12 order of magnitude in frequency, with $f_{\min} = 10^{-6}$ Hz and $f_{\max} = 10^6$ Hz. This safely covers the range in which $1/f$-like charge noise was observed in Si/SiGe QDs.[22,27,35,36] It is also roughly the range of frequencies that contribute to inhomogeneous broadening of splittings of QD-based qubits, for which $f_{\min}$ and $f_{\max}$ are given, roughly, by inverse of total data acquisition time, and single data point measurement time, respectively.

As a result, the density of active TLFs, ρ, is upper-bounded by density of all the interface charges, $\rho_{\mathrm{ic}} \sim 10^{11}\ \mathrm{cm}^{-2}$ (see Ref. 62), as it is not known how many TLFs have γ_n outside of the considered range. Note, however, that the lognormal distribution of γ_n implies a constant number of TLFs per frequency decade, defined as $\mathrm{fpd} = \ln(f_{\max}/f_{\min})/N$. Finally, for a given ρ, we have $N = \rho A$, where $A = 600 \times 600\,\mathrm{nm}^2 \approx 3.6 \times 10^{-10}\mathrm{cm}^2$ is the considered area near of the oxide–semiconductor interface, see Fig. 1.

The initial positions of the TLFs $\{\mathbf{r}_n\}$ are drawn from a uniform spatial distribution. As we assume the displacement vector of each RTN to be independent and isotropic, for each realization we draw components of $\delta\mathbf{r}_n$ from independent normal distributions, $(\delta\mathbf{r}_n)_i = \mathcal{N}(0, \delta r^2/3)$ for $i = x, y, z$, so that the displacement size is approximately δr.

To gauge our results against a measurable quantity, we first concentrate on the variance of the fluctuations of the GS energy, defined as

$$\sigma^2 = 2\int_{f_{\min}}^{f_{\max}} \mathrm{d}f S(f) \approx \sum_{n=1}^{N} \eta_n^2. \tag{4}$$

This quantity is related to the coherence time of the qubit $T_2^* = \alpha\sqrt{2}/\sigma$, where for spin qubits, α is the appropriate lever arm converting electric noise to spin splitting noise due to, e.g., presence of a magnetic field gradient.[26,27,36] For charge qubits, $\alpha \approx 1$, and typically

06 March 2024 09:20:08

Published under an exclusive license by AIP Publishing

measured[63] $T_2^* \approx 0.1$ ns gives $\sigma_0 \approx 8\ \mu$eV. This is confirmed by measured $1/f$ spectrum, with its value at $f_1 = 1$ Hz given by $S_1 \approx 1\mu\text{eV}^2/\text{Hz}$,[56] as we have the relation

$$\sigma^2 = 2\int_{f_{\min}}^{f_{\max}} df S(f) = 2S_1 f_1 \ln\left(\frac{f_{\max}}{f_{\min}}\right) \approx (8\mu\text{eV})^2, \quad (5)$$

where we have used $f_{\max}/f_{\min} = 10^{12}$.

Let us now narrow down the range of possible combinations of ρ and δr that give $\sigma_0 = 8\ \mu$eV. In Fig. 3(a), we show numerically generated distributions of σ as a function of δr for different values of ρ. The considered range of δr covers the values in the few Å range considered in Refs. 25, 39, 64, and 65. The values of ρ correspond to $N \approx 18$, 36, 72 charges in the considered region. In Fig. 3(b), we show that the typical noise amplitude, defined as the ensemble average of σ, scales linearly with δr, i.e., $\langle\sigma\rangle = a_{\text{avg}}(\rho)\delta r$. We highlight that larger δr increases the ensemble variance of noise amplitude $\text{Var}(\sigma) = \langle\sigma^2\rangle - \langle\sigma\rangle^2$. From Fig. 3(c), we conclude that $\sqrt{\text{Var}(\sigma)}$ also scales linearly with δr, i.e., $\sqrt{\text{Var}(\sigma)} \approx a_{\text{std}}(\rho)\delta r$; however, its dependence on ρ is weak.

We investigate the ρ-dependence of $a_{\text{avg}}(\rho)$ and $a_{\text{std}}(\rho)$ in Fig. 4(a), where we plot them for five values of ρ. The match between the results and the linear trend on the log–log scale allows us to extract the exponents γ in $a(\rho) \propto \rho^{\gamma}$. Fitting gives an approximate expression for the ensemble-averaged amplitude,

$$\langle\sigma\rangle = \left[c_0\left(\frac{\rho}{10^{10}\text{cm}^{-2}}\right)^{\gamma_{avg}} + a_{avg,0}\right]\frac{\delta r}{\text{nm}}\mu\text{eV}, \quad (6)$$

where $c_0 = 59.2$ and $a_{\text{avg},0} = 0.951$. In Fig. 4(b), we plot Eq. (6) as a function of ϱ and δr. Black line shows the set of parameters resulting in $\langle\sigma\rangle = \sigma_0 = 8\ \mu$eV. Close to this line, we mark four points, which are used to generate the PSDs in Fig. 5.

In Fig. 4, we also prove that $\text{Var}(\sigma)$ does not depend visibly on ρ, see an almost horizontal red line in Fig. 4. Consequently, in the

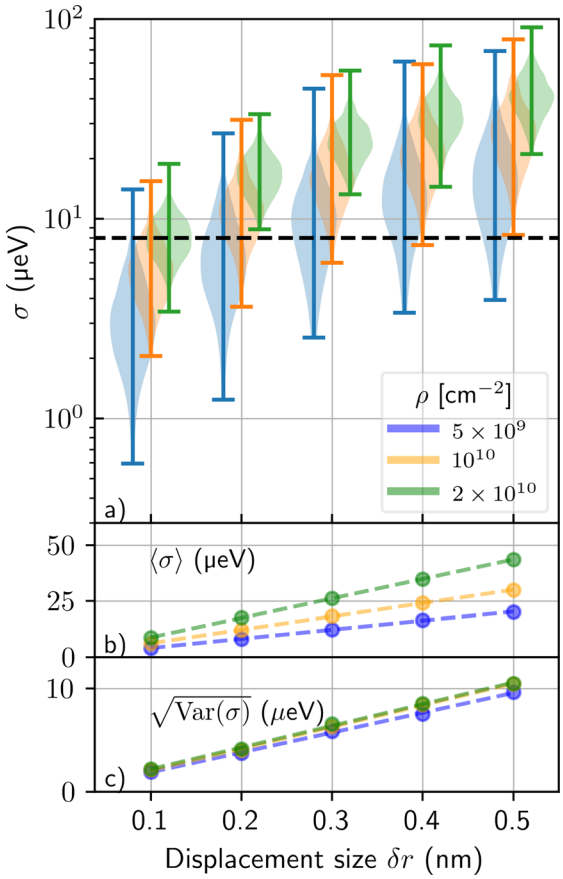

FIG. 3. Statistics of the amplitude of the noise, for different charge densities ρ and magnitudes of charge displacement, δr. (a) The distribution of noise amplitude from 1000 realizations for $\delta r = 0.1, 0.2, 0.3, 0.4, 0.5$ nm (x-axis) and $\rho = 5 \times 10^9$, $10^{10}, 2 \times 10^{10}$ cm^{-2} (colors). Black dashed line corresponds to the targeted $\sigma_0 = 8\ \mu$eV. (b) Ensemble averaged noise amplitude, $\langle\sigma\rangle$ and (c) standard deviation of noise amplitude over the ensemble $\sqrt{\text{Var}(\sigma)} = \sqrt{\langle\sigma^2\rangle - \langle\sigma\rangle^2}$, both as a function of δr for three charge densities from (a), with linear trends marked by dashed lines.

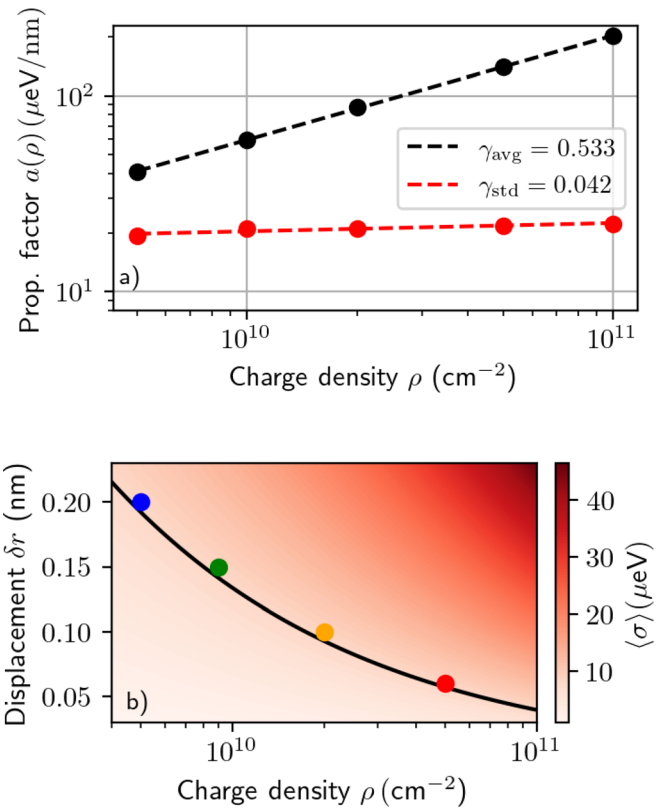

FIG. 4. Noise amplitude as a function of ρ and δr. (a) Proportionality factor of the ensemble average of noise amplitude $\langle\sigma\rangle \propto a_{\text{avg}}(\rho)\delta r$ (black) and corresponding ensemble variance $\sqrt{\langle\sigma^2\rangle - \langle\sigma\rangle^2} \propto a_{\text{std}}(\rho)\delta r$ (red). Points correspond to the numerical results obtained by averaging 1000 realizations, and dashed-lines are the linear fit on the log scale. From the fit, we identify the corresponding exponents $a(\rho) \propto \rho^{\gamma}$ (see the legend for their values). (b) The fitted formula, Eq. (6), as a function of ρ and δr. Black line corresponds to $\langle\sigma\rangle = \sigma_0 = 8\ \mu$eV, and dots denote sets of parameters used to plot spectral densities in Fig. 5.

06 March 2024 09:20:08

Published under an exclusive license by AIP Publishing

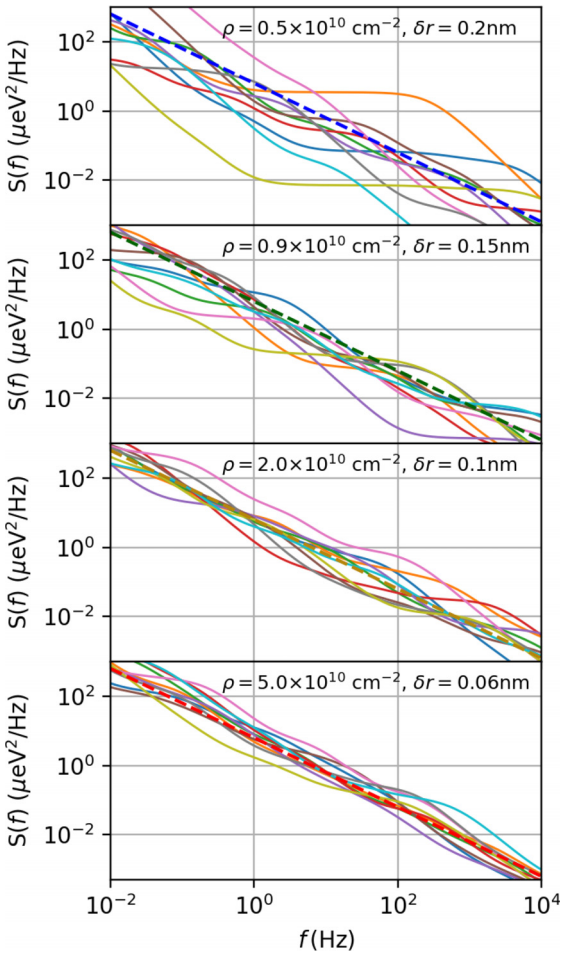

FIG. 5. Random realizations of power spectral densities for a selection of displacement magnitudes, δr, and charge densities, ρ, which result in a typical noise amplitude σ_0. The dashed lines are the ideal $1/f$ noise with $S_1 = 1\,\mu\text{eV}^2/\text{Hz}$, and their color is related to points marked in Fig. 4(b). The solid lines are used to plot 10 realizations of TLF positions and their displacement for each set of parameters.

relevant range of ρ, it is given by $\sqrt{\text{Var}(\sigma)} \approx a_{\text{std},0}\delta r$, where $a_{\text{std},0} \approx 20\mu\text{eV/nm}$. This Var (σ) is related to variability between statistically equivalent devices, which determines the reproducibility of QD properties and, thus, the yield of usable devices.[66]

Finally, we use the above analysis and the obtained couplings $\{\eta_n\}$ to generate the noise PSDs, defined via Eq. (1). We concentrate on pairs $(\rho, \delta r)$ that reproduce $\langle\sigma\rangle \approx 8\ \mu\text{eV}$ [the points in Fig. 4(b)]. In Fig. 5, we plot 10 realizations of the PSD and compare them with a model $1/f$ noise spectrum with $S_1 = 1\,\mu\text{eV/Hz}$ (dashed lines) for each point marked in Fig. 4(b). Unsurprisingly, for all the sets we recover the PSD at 1 Hz to be approximately 1 $\mu\text{eV}^2/\text{Hz}$. However, for smallest $\rho = 5 \times 10^9\ \text{cm}^{-2}$ (fpd ≈ 1.5) and largest considered $\delta r = 0.2\,\text{nm}$, in the uppermost panel of Fig. 4, we see very strong effects of discrete number of TLFs, reflected in a locally Lorentzian PSD. While such strong single-TLF effects were seen in some experiments,[27,35,36,67] the PSD recently observed in Ref. 68 is more closely matched by the results of the second panel, where $\rho \approx 10^{10}\ \text{cm}^{-2}$ and fpd ≈ 2.7, for which flat regions of PSD are less likely. The third panel (fpd ≈ 6) typically shows $S(f) \sim 1/f^{\alpha}$ with non-constant exponent $\alpha < 2$ and resembles other experimentally measured PSDs.[22,27,36] Finally, in the fourth panel, we have results with $\alpha \approx 1$, i.e., spectra close to the ideal $1/f$ behavior.

In summary, we have calculated electrostatic couplings between a quantum dot defined in realistic Si/SiGe nanostructure, and the charges trapped in the oxide above the semiconductor layer. Starting with reasonable initial ranges, parameters for isotropic displacements of these charges, δr, and their densities, ρ, we have identified a set of $(\rho, \delta r)$ pairs, for which in the typically observed amplitude of $1/f$ charge noise at 1 Hz, and its total power can be reproduced. Deviations from an ideal $1/f$ shape of charge noise PSDs measured in various Si/SiGe structures[22,27,35,36,67,68] can be reproduced with $\rho \geq 10^{10}\ \text{cm}^{-2}$ and $\delta r \leq 0.15$ nm. Note that these numbers might differ from actual values of ρ and δr, as the QDs that work well as spin qubits could be subjected to selection bias, i.e., focusing on QDs with lower-than typical amplitude of noise. The ranges of parameters found here to be consistent with experiments can be further narrowed down if more information on noise in a given nanostructure—for example on cross-correlations of noises in two QDs[36]—is available. Note that a recent paper[68] shows that those correlations can be obtained in a model with ρ similar to the one obtained here. Using the model and the parameter ranges identified here to calculation of PSD of spin splitting noise for a given direction of magnetic field gradient is left for the future work.

This research was funded in whole by National Science Centre, Poland, Grant No. 2021/41/N/ST3/02758.

AUTHOR DECLARATIONS

Conflict of Interest

The authors have no conflicts to disclose.

Author Contributions

Marcin Kępa: Investigation (equal); Software (lead); Visualization (lead); Writing – review & editing (equal). **Niels Focke:** Methodology (supporting); Software (supporting); Writing – review & editing (supporting). **Lukasz Cywinski:** Conceptualization (equal); Methodology (equal); Writing – review & editing (equal). **Jan Adrian Krzywda:** Conceptualization (equal); Funding acquisition (lead); Investigation (equal); Methodology (equal); Project administration (lead); Software (equal); Writing – original draft (lead); Writing – review & editing (equal).

DATA AVAILABILITY

The data that support the findings of this study are available from the corresponding author upon reasonable request.

REFERENCES

[1]P. Dutta and P. M. Horn, Rev. Mod. Phys. **53**, 497 (1981).
[2]E. Paladino, Y. M. Galperin, G. Falci, and B. L. Altshuler, Rev. Mod. Phys. **86**, 361 (2014).
[3]D. M. Fleetwood, IEEE Trans. Nucl. Sci. **62**, 1462 (2015).
[4]S. Islam, S. Shamim, and A. Ghosh, Adv. Mater. **35**, 2109671 (2023).
[5]B. P. Wuetz, D. D. Esposti, A. M. J. Zwerver, S. V. Amitonov, M. Botifoll, J. Arbiol, A. Sammak, L. M. K. Vandersypen, M. Russ, and G. Scappucci, Nat. Commun. **14**, 1385 (2023).

06 March 2024 09:20:08

Published under an exclusive license by AIP Publishing

[6]T. Sakamoto, Y. Nakamura, and K. Nakamura, Appl. Phys. Lett. **67**, 2220–2222 (1995).
[7]F. Liefrink, J. I. Dijkhuis, and H. V. Houten, Semicond. Sci. Technol. **9**, 2178–2189 (1994).
[8]G. Ramon and X. Hu, Phys. Rev. B **81**, 045304 (2010).
[9]A. Bermeister, D. Keith, and D. Culcer, Appl. Phys. Lett. **105**, 192102 (2014).
[10]R. Hanson, L. P. Kouwenhoven, J. R. Petta, S. Tarucha, and L. M. K. Vandersypen, Rev. Mod. Phys. **79**, 1217 (2007).
[11]G. Burkard, T. D. Ladd, J. M. Nichol, A. Pan, and J. R. Petta, arXiv:2112.08863 (2021).
[12]S. G. J. Philips, M. T. Madzik, S. V. Amitonov, S. L. de Snoo, M. Russ, N. Kalhor, C. Volk, W. I. L. Lawrie, D. Brousse, L. Tryputen, B. P. Wuetz, A. Sammak, M. Veldhorst, G. Scappucci, and L. M. K. Vandersypen, Nature **609**, 919 (2022).
[13]F. Borsoi, N. W. Hendrickx, V. John, S. Motz, F. van Riggelen, A. Sammak, S. L. de Snoo, G. Scappucci, and M. Veldhorst, arXiv:2209.06609 (2022).
[14]P. Huang, N. M. Zimmerman, and G. W. Bryant, npj Quantum Inf. **4**, 62 (2018).
[15]M. Veldhorst, C. H. Yang, J. C. C. Hwang, W. Huang, J. P. Dehollain, J. T. Muhonen, S. Simmons, A. Laucht, F. E. Hudson, K. M. Itoh, A. Morello, and A. S. Dzurak, Nature **526**, 410 (2015).
[16]D. M. Zajac, A. J. Sigillito, M. Russ, F. Borjans, J. M. Taylor, G. Burkard, and J. R. Petta, Science **359**, 439 (2018).
[17]T. F. Watson, S. G. J. Philips, E. Kawakami, D. R. Ward, P. Scarlino, M. Veldhorst, D. E. Savage, M. G. Lagally, M. Friesen, S. N. Coppersmith, M. A. Eriksson, and L. M. K. Vandersypen, Nature **555**, 633 (2018).
[18]W. A. Coish and D. Loss, Phys. Rev. B **72**, 125337 (2005).
[19]X. Hu and S. Das Sarma, Phys. Rev. Lett. **96**, 100501 (2006).
[20]O. E. Dial, M. D. Shulman, S. P. Harvey, H. Bluhm, V. Umansky, and A. Yacoby, Phys. Rev. Lett. **110**, 146804 (2013).
[21]K. Takeda, A. Noiri, J. Yoneda, T. Nakajima, and S. Tarucha, Phys. Rev. Lett. **124**, 117701 (2020).
[22]E. J. Connors, J. Nelson, L. F. Edge, and J. M. Nichol, Nat. Commun. **13**, 940 (2022).
[23]K. W. Chan, W. Huang, C. H. Yang, J. C. Hwang, B. Hensen, T. Tanttu, F. E. Hudson, K. M. Itoh, A. Laucht, A. Morello, and A. S. Dzurak, Phys. Rev. Appl. **10**, 044017 (2018).
[24]Z. Qi, X. Wu, D. R. Ward, J. R. Prance, D. Kim, J. K. Gamble, R. T. Mohr, Z. Shi, D. E. Savage, M. G. Lagally, M. A. Eriksson, M. Friesen, S. N. Coppersmith, and M. G. Vavilov, Phys. Rev. B **96**, 115305 (2017).
[25]D. Culcer and N. M. Zimmerman, Appl. Phys. Lett. **102**, 232108 (2013).
[26]J. Yoneda, K. Takeda, T. Otsuka, T. Nakajima, M. R. Delbecq, G. Allison, T. Honda, T. Kodera, S. Oda, Y. Hoshi, N. Usami, K. M. Itoh, and S. Tarucha, Nat. Nanotechnol. **13**, 102 (2018).
[27]T. Struck, A. Hollmann, F. Schauer, O. Fedorets, A. Schmidbauer, K. Sawano, H. Riemann, N. V. Abrosimov, Ł. Cywiński, D. Bougeard, and L. R. Schreiber, npj Quantum Inf. **6**, 40 (2020).
[28]A. Saraiva, W. H. Lim, C. H. Yang, C. C. Escott, A. Laucht, and A. S. Dzurak, Adv. Funct. Mater. **32**, 2105488 (2022).
[29]W. Gilbert, T. Tanttu, W. H. Lim, M. Feng, J. Y. Huang, J. D. Cifuentes, S. Serrano, P. Y. Mai, R. C. C. Leon, C. C. Escott, K. M. Itoh, N. V. Abrosimov, H.-J. Pohl, M. L. W. Thewalt, F. E. Hudson, A. Morello, A. Laucht, C. H. Yang, A. Saraiva, and A. S. Dzurak, Nat. Nanotechnol. **18**, 131–136 (2023).
[30]P. Harvey-Collard, N. T. Jacobson, C. Bureau-Oxton, R. M. Jock, V. Srinivasa, A. M. Mounce, D. R. Ward, J. M. Anderson, R. P. Manginell, J. R. Wendt, T. Pluym, M. P. Lilly, D. R. Luhman, M. Pioro-Ladrière, and M. S. Carroll, Phys. Rev. Lett. **122**, 217702 (2019).
[31]T. Tanttu, B. Hensen, K. W. Chan, C. H. Yang, W. W. Huang, M. Fogarty, F. Hudson, K. Itoh, D. Culcer, A. Laucht, A. Morello, and A. Dzurak, Phys. Rev. X **9**, 021028 (2019).
[32]K. Takeda, A. Noiri, T. Nakajima, T. Kobayashi, and S. Tarucha, Nature **608**, 682 (2022).
[33]K. Takeda, J. Kamioka, T. Otsuka, J. Yoneda, T. Nakajima, M. R. Delbecq, S. Amaha, G. Allison, T. Kodera, S. Oda, and S. Tarucha, Sci. Adv. **2**, e1600694 (2016).
[34]R. Brunner, Y.-S. Shin, T. Obata, M. Pioro-Ladrière, T. Kubo, K. Yoshida, T. Taniyama, Y. Tokura, and S. Tarucha, Phys. Rev. Lett. **107**, 146801 (2011).
[35]E. J. Connors, J. Nelson, H. Qiao, L. F. Edge, and J. M. Nichol, Phys. Rev. B **100**, 165305 (2019).
[36]J. Yoneda, J. S. Rojas-Arias, P. Stano, K. Takeda, A. Noiri, T. Nakajima, D. Loss, and S. Tarucha, arXiv:2208.14150 (2022).
[37]K. D. Petersson, J. R. Petta, H. Lu, and A. C. Gossard, Phys. Rev. Lett. **105**, 246804 (2010).
[38]X. Mi, S. Kohler, and J. R. Petta, Phys. Rev. B **98**, 161404 (2018).
[39]M. M. E. K. Shehata, G. Simion, R. Li, F. A. Mohiyaddin, D. Wan, M. Mongillo, B. Govoreanu, I. Radu, K. De Greve, and P. Van Dorpe, arXiv:2210.04539 (2022).
[40]B. Shalak, C. Delerue, and Y.-M. Niquet, arXiv:2210.10476 (2022).
[41]I. Seidler, T. Struck, R. Xue, N. Focke, S. Trellenkamp, H. Bluhm, and L. R. Schreiber, npj Quantum Inf. **8**, 100 (2022).
[42]V. Langrock, J. A. Krzywda, N. Focke, I. Seidler, L. R. Schreiber, and Ł. Cywiński, arXiv:2202.11793 (2022).
[43]J. Klos, F. Hassler, P. Cerfontaine, H. Bluhm, and L. R. Schreiber, Phys. Rev. B **98**, 155320 (2018).
[44]J. Klos, B. Sun, J. Beyer, S. Kindel, L. Hellmich, J. Knoch, and L. R. Schreiber, Appl. Sci. **9**, 3823 (2019).
[45]P. C. Spruijtenburg, S. V. Amitonov, F. Mueller, W. G. van der Wiel, and F. A. Zwanenburg, Sci. Rep. **6**, 38127 (2016).
[46]N. H. Thoan, K. Keunen, V. V. Afanas'ev, and A. Stesmans, J. Appl. Phys. **109**, 013710 (2011).
[47]J. P. Campbell, P. M. Lenahan, A. T. Krishnan, and S. Krishnan, Appl. Phys. Lett. **87**, 204106 (2005).
[48]S. Machlup, J. Appl. Phys. **25**, 341 (1954).
[49]M. Constantin, C. C. Yu, and J. M. Martinis, Phys. Rev. B **79**, 094520 (2009).
[50]J. Schriefl, Y. Makhlin, A. Shnirman, and G. Schön, New J. Phys. **8**, 1 (2006).
[51]X. You, A. A. Clerk, and J. Koch, Phys. Rev. Res. **3**, 013045 (2021).
[52]A. Shnirman, G. Schön, I. Martin, and Y. Makhlin, Phys. Rev. Lett. **94**, 127002 (2005).
[53]C. Müller, J. H. Cole, and J. Lisenfeld, Rep. Prog. Phys. **82**, 124501 (2019).
[54]F. Beaudoin and W. A. Coish, Phys. Rev. B **91**, 165432 (2015).
[55]S. Ahn, S. Das Sarma, and J. P. Kestner, Phys. Rev. B **103**, L041304 (2021).
[56]L. Kranz, S. K. Gorman, B. Thorgrimsson, Y. He, D. Keith, J. G. Keizer, and M. Y. Simmons, Adv. Mater. **32**, 2003361 (2020).
[57]A. R. Mills, C. R. Guinn, M. J. Gullans, A. J. Sigillito, M. M. Feldman, E. Nielsen, and J. R. Petta1, Sci. Adv. **8**, eabn5130 (2022).
[58]D. M. Zajac, T. M. Hazard, X. Mi, K. Wang, and J. R. Petta, Appl. Phys. Lett. **106**, 223507 (2015).
[59]M. G. Borselli, K. Eng, R. S. Ross, T. M. Hazard, K. S. Holabird, B. Huang, A. A. Kiselev, P. W. Deelman, L. D. Warren, I. Milosavljevic, A. E. Schmitz, M. Sokolich, M. F. Gyure, and A. T. Hunter, Nanotechnology **26**, 375202 (2015).
[60]B. Paquelet Wuetz, M. P. Losert, S. Koelling, L. E. A. Stehouwer, A.-M. J. Zwerver, S. G. J. Philips, M. T. Madzik, X. Xue, G. Zheng, M. Lodari, S. V. Amitonov, N. Samkharadze, A. Sammak, L. M. K. Vandersypen, R. Rahman, S. N. Coppersmith, O. Moutanabbir, M. Friesen, and G. Scappucci, Nat. Commun. **13**, 7730 (2022).
[61]N. Holman, D. Rosenberg, D. Yost, J. L. Yoder, R. Das, W. D. Oliver, R. McDermott, and M. A. Eriksson, npj Quantum Inf. **7**, 137 (2021).
[62]J. Zimmermann and G. Weber, Phys. Rev. Lett. **46**, 661 (1981).
[63]Z. Shi, C. B. Simmons, D. R. Ward, J. R. Prance, R. T. Mohr, T. S. Koh, J. K. Gamble, X. Wu, D. E. Savage, M. G. Lagally, M. Friesen, S. N. Coppersmith, and M. A. Eriksson, Phys. Rev. B **88**, 075416 (2013).
[64]J. Reinisch and A. Heuer, arXiv:cond-mat/0609693 (2006).
[65]R. Biswas and Y.-P. Li, Phys. Rev. Lett. **82**, 2512 (1999).
[66]A. M. J. Zwerver, T. Krähenmann, T. F. Watson, L. Lampert, H. C. George, R. Pillarisetty, S. A. Bojarski, P. Amin, S. V. Amitonov, J. M. Boter, R. Caudillo, D. Correas-Serrano, J. P. Dehollain, G. Droulers, E. M. Henry, R. Kotlyar, M. Lodari, F. Lüthi, D. J. Michalak, B. K. Mueller, S. Neyens, J. Roberts, N. Samkharadze, G. Zheng, O. K. Zietz, G. Scappucci, M. Veldhorst, L. M. K. Vandersypen, and J. S. Clarke, Nat. Electron. **5**, 184 (2022).
[67]S. Kafanov, H. Brenning, T. Duty, and P. Delsing, Phys. Rev. B **78**, 125411 (2008).
[68]J. S. Rojas-Arias, A. Noiri, P. Stano, T. Nakajima, J. Yoneda, K. Takeda, T. Kobayashi, A. Sammak, G. Scappucci, D. Loss, and S. Tarucha, arXiv:2302.11717 (2023).

06 March 2024 09:20:08

Published under an exclusive license by AIP Publishing